



HAL
open science

Beamix: Application of an Ambisonics filter bank for the creation of directional effects

Thibaut Carpentier

► **To cite this version:**

Thibaut Carpentier. Beamix: Application of an Ambisonics filter bank for the creation of directional effects. Sound and Music Computing (SMC), Jul 2024, Porto, Portugal. hal-04646935

HAL Id: hal-04646935

<https://hal.science/hal-04646935v1>

Submitted on 12 Jul 2024

HAL is a multi-disciplinary open access archive for the deposit and dissemination of scientific research documents, whether they are published or not. The documents may come from teaching and research institutions in France or abroad, or from public or private research centers.

L'archive ouverte pluridisciplinaire **HAL**, est destinée au dépôt et à la diffusion de documents scientifiques de niveau recherche, publiés ou non, émanant des établissements d'enseignement et de recherche français ou étrangers, des laboratoires publics ou privés.



Distributed under a Creative Commons Attribution 4.0 International License

BEAMIX : APPLICATION OF AN AMBISONICS FILTER BANK FOR THE CREATION OF DIRECTIONAL EFFECTS

Thibaut CARPENTIER (thibaut.carpentier@ircam.fr)¹

¹STMS Lab, IRCAM — CNRS — Sorbonne Université — Ministère de la Culture, 1, place Igor-Stravinsky, Paris, 75004 France

ABSTRACT

In this article we present `beamix`, an audio engine and its graphical user interface which allow one to produce directional audio effects (FX), that is, sound transformations localized in certain areas of space. These effects (such as equalizer, compressor, etc.) are applied to an Ambisonics-encoded sound scene, which was previously decomposed by a spatial filter bank. The latter, based on the state of the art, applies beamforming with virtual microphones (a process analogous to a plane-wave decomposition of the sound field) so as to partition the 3D or 2D sound field into a set of angular sectors. A chain of audio effects can be inserted into each of these sectors, allowing fine manipulation of the soundscape. The approach thus proposed offers more flexibility than transformations applied in the spherical harmonics domain, in particular for the realization of non-linear effects. The tool is typically useful for production or post-production of Ambisonics scenes, but can also be used for editing directional room impulse responses (DRIR).

1. INTRODUCTION

1.1 Filter bank

In signal processing, a filter bank refers to a set of K band-pass filters that decompose an input signal x into K components, each representing a frequency sub-band. This is ubiquitously used in the field of computer music to achieve *multiband* effects [1, Section 2.6.3], such as graphic equalizers (EQ) or multiband dynamic compression (compressor/expander). An important property of filter banks is their ability correctly to *reconstruct* the input signal. Perfect reconstruction is achieved when the output signal y is such that $y[n] = x[n]$ when no effect is applied.

1.2 Spatial filter bank

A *spatial* filter bank is conceptually similar, except that the input signal x is not a monophonic signal but a spatial sound field, and the filtering operates in the angular domain (azimuth and/or elevation angles) rather than in the frequency domain. In other words, a spatialized sound scene — represented in 3D on the surface of a sphere, or in 2D on a circle

— is decomposed into a set of sectors forming a partition of space. Filtering in the spatial domain can be achieved by a beamforming technique that consists of synthesizing virtual microphones with adjustable characteristics (steering direction and directivity pattern) [2, 3].

1.3 Spatial filter bank in Ambisonics

Ambisonics is a recording and reproduction technique that can be used to create spatial sound for circular or spherical loudspeaker arrangements [4, 5]. The technique is based on the representation of the sound field as a combination of orthogonal basis functions, namely the spherical harmonics (SH). The spatial filtering operation (i.e. beamforming) can be elegantly and efficiently designed in the SH domain [6, 7], effectively decomposing an Ambisonics scene into different angular sectors.

Such partitioning is typically used for local *analysis* of the sound field, in particular to estimate the acoustic intensity or energy density [8, 9], to improve estimation techniques of directions of arrival [10], to analyze the directional properties of a reverberant field [11–16], to visualize activity maps [17], or to implement audio compression algorithms for bandwidth reduction [18]. More generally, spatial filter banks are potentially useful for *parametric* spatial processing methods [19], such as DirAC [20], Harpex [21], HO-DirAC [18, 22–24], Spare Recovery [25], or COMPASS [26].

The above-mentioned techniques are mainly concerned with the *analysis* or reproduction of the sound field. In the present study, we focus on the exploitation of Ambisonics filter banks for the creation of audio effects, i.e. for the *transformation* of the sound scene, typically for artistic production (or post-production) applications.

The principle of the approach is illustrated in Figure 1: the incoming Ambisonics stream x is decomposed into K angular sectors by a filter bank derived from [18, 27, 28], and which is similar to a plane-wave decomposition (PWD) of the sound field [29]. After processing with various monophonic effects, the output stream y is recomposed by re-encoding the K plane waves, in the K analyzed directions, in the Ambisonics domain.

1.4 Ambisonics FX

Transforming a sound field by applying FX to an Ambisonics stream is not a new approach. Various tools are already available to sound engineers and composers. Some of these FX are operated globally on the sound scene, by

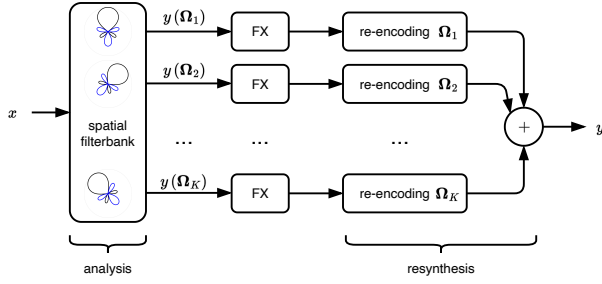


Figure 1. Proposed framework for the implementation of spatially localized audio FX.

application of a (frequency-independent) transformation matrix to the Ambisonics stream [30] [5, Chapter 5.2]; this includes in particular the rotation [4, 31], mirror [32], or spatial blur [33] effects. Other FX were first formulated in the spatial domain, then “translated” into the modal domain by discrete SH transform [34]; this methodology is fundamentally similar to the analysis/resynthesis filter bank shown in Figure 1. However, the filter bank approach may prove more intuitive for certain users, in particular sound engineers who easily understand the concept of virtual microphones. This strategy (of design in the spatial domain) notably makes it possible to design higher-order FX such as directional emphasis (or directional loudness) [34] and angular distortion (also known as dominance [32, 35] or warping [5, 36]). Another extension of these methods, based on PWD, was proposed by Hafsaty et al. [37] in order to produce even more “fine” editing of the sound scene; the technique however relies on the assumption that the directions of S sources of interest are known (or have been previously estimated).

This article is organized as follows: in Section 2, we recall the theoretical background for the creation of a perfect reconstruction Ambisonics filter bank. In Section 3 we present the software tool `beamix` which implements such a filter bank. Consisting of an audio engine associated with a graphical user interface, the tool extends the transformation possibilities of the approaches cited above, while offering intuitive control.

2. BACKGROUND

This section briefly summarizes the spatial filter bank approach proposed by Hold et al. [18, 27, 28].

2.1 Axis-symmetric beamforming

Here we consider Ambisonics signals encoded on a basis of spherical harmonics $Y_n^m(\Omega)$, with N denoting the maximum order. $\Omega \equiv (\theta, \phi)$ denotes the angular direction in the spherical coordinate system. The spherical harmonic addition theorem [7, Eq. 1.26] is written $\forall \Omega, \Omega' \in \mathbb{S}^2$:

$$\sum_{m=-n}^n [Y_n^m(\Omega)]^* Y_n^m(\Omega') = \frac{2n+1}{\lambda^2} \mathcal{P}_n(\cos \Theta), \quad (1)$$

where \mathcal{P}_n is the Legendre polynomial of order n , and $\Theta = \angle(\Omega, \Omega')$ represents the angle between the directions Ω and Ω' . λ here denotes a constant which depends only on the chosen variety of SH. In the case of N3D normalization, guaranteeing the orthonormality of the components [4, 38], we have $\lambda^2 = 1$; however most publications [5, 7, 28, 29, 39] adopt the convention $\lambda^2 = 4\pi$. For the sake of compatibility, we keep the generic notation λ in the formulas that follow.

It follows from the addition theorem that any axis-symmetric directional function, obtained by weighting the SH with $(N+1)$ real coefficients d_n , can be expressed in the form [40] [7, Eq. 5.24]:

$$y(\Theta) = \sum_{n=0}^N d_n \frac{2n+1}{\lambda^2} \mathcal{P}_n(\cos \Theta). \quad (2)$$

This expression characterizes the output signal $y(\Theta)$ resulting from a modal beamforming operation.

2.2 Choice of spatial sampling

To create the spatial filter bank, we use K beamformers pointing in directions $\{\Omega_k\}$ for $k = 1, \dots, K$. These directions must be “uniformly” distributed, so as to ensure numerical quadrature over \mathbb{S}^2 . Assuming a uniform distribution, the integration of a band-limited continuous function $f \in \mathbb{S}^2$ reduces to a discrete summation:

$$\int_{\mathbb{S}^2} f(\Omega) d\Omega = \frac{\lambda^2}{K} \sum_{k=1}^K f(\Omega_k). \quad (3)$$

The spherical t -design sampling schemes [41, 42] are known to satisfy this quadrature condition (Eq. 3), provided that $t \geq (2N+1)$ [5, Section 4.7] [7, Section 3.4]. From now on, we assume that $\{\Omega_k\}$ is such a spherical t -design arrangement. To evaluate the reconstruction capacity of the spatial filter bank, we are interested in the sum of the contributions of the K sectors, which we can write:

$$\begin{aligned} \sum_{k=1}^K y(\Theta_k) &= \sum_{k=1}^K \sum_{n=0}^N d_n \frac{2n+1}{\lambda^2} \mathcal{P}_n(\cos \Theta_k) \\ &= \sum_{k=1}^K \sum_{n=0}^N d_n \sum_{m=-n}^n [Y_n^m(\Omega)]^* Y_n^m(\Omega_k) \\ &= \sum_{n=0}^N d_n \sum_{m=-n}^n [Y_n^m(\Omega)]^* \sum_{k=1}^K Y_n^m(\Omega_k) \end{aligned} \quad (4)$$

(the spherical addition theorem Eq. 1 has been introduced between the first and second lines). Furthermore, by applying the quadrature equation Eq. 3 to the $Y_n^m(\Omega_k)$ function, we have:

$$\sum_{k=1}^K Y_n^m(\Omega_k) = \frac{K}{\lambda^2} \int_{\mathbb{S}^2} Y_n^m(\Omega) d\Omega. \quad (5)$$

By virtue of the SH orthogonality, we know that:

$$\int_{\mathbb{S}^2} Y_n^m(\Omega) d\Omega = \lambda \delta_{n0}, \quad (6)$$

where δ_{nm} represents the Kronecker symbol ($\delta_{nm} = 1$ if $n = m$, 0 otherwise). We can thus simplify the summation equation Eq. 4 over the K sectors:

$$\sum_{k=1}^K y(\Theta_k) = d_0 [Y_0^0(\Omega)]^* \frac{K}{\lambda} = d_0 \frac{K}{\lambda^2}, \quad (7)$$

since $\forall \Omega \in \mathbb{S}^2$, $Y_0^0(\Omega) = \lambda^{-1}$, by construction.

2.3 Energy or amplitude compensation

As discussed in [18, 27, 28], it is necessary to introduce a scaling factor to ensure the perfect reconstruction of the filter bank. When amplitude reconstruction is needed, we introduce a factor β_A which must satisfy $\forall \Omega \in \mathbb{S}^2$, $\sum_{k=1}^K \beta_A y(\Omega_k) = 1$. Comparing this with Eq. 7, it follows that $\beta_A = \frac{\lambda^2}{d_0 K}$ is a solution. When energy reconstruction is desired, we must introduce a factor β_E such that $\forall \Omega \in \mathbb{S}^2$, $\sum_{k=1}^K \beta_E y^2(\Omega_k) = 1$, and it is easily shown that $\beta_E = \frac{\lambda^2}{d_0^2 K}$. These compensation factors are introduced into the resynthesis stage (Figure 1) in order to ensure the perfect reconstruction of the filter bank (see [18, Sections III.A.5 and III.A.6] for more details).

2.4 Choice of the beampattern

After choosing the directions $\{\Omega_k\}$, one needs to determine the directivity pattern (i.e. the selectivity) of the beamformer. A natural choice is the hyper-cardioid beampattern of order N , as it performs a PWD of the sound field [7, 29]. It is realized using constant modal weights such that [40] [7, Eq. 6.10]:

$$\forall n \leq N, d_n = \frac{4\pi}{(N+1)^2}. \quad (8)$$

The resulting directivity pattern is also called a ‘‘regular beampattern’’ or ‘‘basic’’ (in Ambisonics vernacular), and it achieves the maximum directivity index [7, 40]. Despite this interesting property, the hyper-cardioid pattern can be criticized because it exhibits strong sidelobes (lateral and rear). This point is particularly sensitive when creating a spatial filter bank because the sidelobes of the K beams interfere. Therefore, other beampatterns may be preferred; among the different commonly used options, we can for example retain two of interest: (a) the cardioid pattern (also referred to as ‘‘in-phase’’ in Ambisonics dialect) which is designed to suppress signals arriving in the opposite direction ($\Theta = \pm 180^\circ$) while providing an optimally flat response in that direction. The response of the cardioid beamformer satisfies [43, Section 6.1]:

$$y(\Theta) = \left(\frac{1 + \cos \Theta}{2} \right)^N, \quad (9)$$

and it is achieved with the weights [4, Eq. 3.91]:

$$\forall n \leq N, d_n = 4\pi \frac{(N!)^2}{(N+n+1)!(N-n)!}. \quad (10)$$

(b) The so-called max- r_E pattern is also interesting because, as the name suggests, it is designed to maximize the norm

r_E of the energy vector [4, 5]. The properties of this beampattern are somewhat similar to the super-cardioid pattern (providing the maximum front-to-back ratio). The max- r_E weighting is given by [4, Eq. 3.89]:

$$\forall n \leq N, d_n = \mathcal{P}_n(r_E(N)), \quad (11)$$

where $r_E(N)$ is the largest root of $\mathcal{P}_{N+1}(\cdot)$; this can be approximated by $r_E(N) \approx \cos\left(\frac{137.9^\circ}{N+1.52}\right)$ (see [5, Section A.3.7]).

3. IMPLEMENTATION

3.1 Description of the tool

The processing chain proposed in Figure 1 is implemented in the C++ language in the form of two external objects for the Max environment¹. The `spat5.hoa.beamix~` object renders the signal processing, and the `spat5.hoa.beamix` object is the associated graphical user interface (GUI), developed with the Juce framework². The objects are integrated into the Spat library [44], distributed free of charge by Ircam³.

The GUI is shown in Figure 5. The left part shows a map projection of the sphere \mathbb{S}^2 ; different types of projection are available, and by default the Mollweide projection is used. The meridians and parallels are displayed in light gray. The K angular sectors are represented (here in blue); their index is placed at the center of the area, and the sectors are delimited by the edges of the corresponding spherical Voronoi diagram. In the example of Figure 5, sector #17 (in red) is currently selected by the user. The right half of the interface shows the effects controllers for the selected area(s). Currently implemented are traditional audio effects, namely gain and delay adjustment, parametric EQ (with 8 adjustable stages) and compressor/expander. To complete this toolchain, it is also possible to load (from an audio file) a finite impulse response filter which is rendered by an optimized convolution engine. Finally it is possible to mute or solo the sector, which is typically useful when tweaking the FX settings. Vu-meters display the input (pre-FX) and output (post-FX) levels of the sector.

In the case of a 2D Ambisonics scene, a polar representation of the directional beams is displayed (Figure 2) instead of the map projection (Figure 5, left).

3.2 Adjustable beampattern

In Figure 2 (with $N = 3$, $K = 7$, and hyper-cardioid patterns), we clearly observe the role of the sidelobes which significantly ‘‘leak’’ into all other sectors. As mentioned in Section 2.4, this sometimes motivates the use of alternative beampatterns with less pronounced sidelobes (but therefore with lower selectivity), such as *in-phase* or max- r_E . In `spat5.hoa.beamix`, to facilitate user experience, the selectivity of the beamformer is adjustable with a continuous parameter α , allowing a tradeoff between cardioid ($\alpha = 0\%$), max- r_E ($\alpha = 50\%$) and hyper-cardioid

¹ <https://cycling74.com>

² <https://juce.com>

³ <https://forum.ircam.fr/projects/detail/spat/>

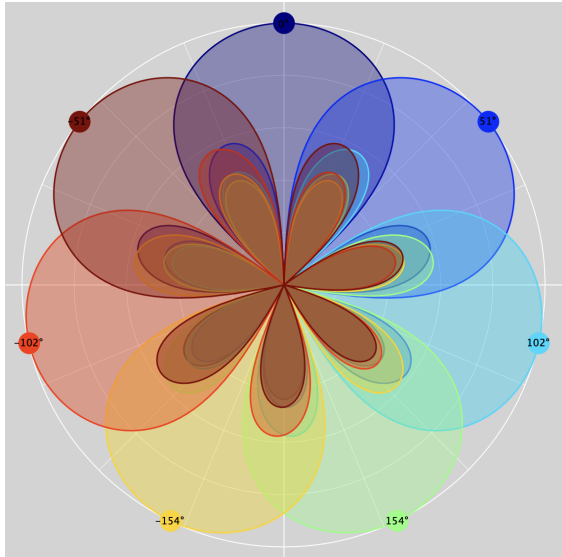


Figure 2. `spat5.hoa.beamix` filter bank (polar plot of hyper-cardioid beampatterns) in the 2D case. Here for $N = 3$, therefore $K = 7$ beams. The radial scale is logarithmic, with 6 dB per division.

($\alpha = 100\%$) beampatterns. The transition between these three diagrams is made by linear interpolation between the weights d_n , with an approach similar to [45]. Figure 3 illustrates the polar diagram of the beamformer for different values of α .

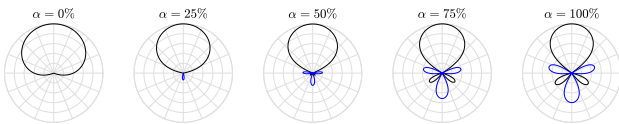


Figure 3. Directivity pattern with adjustable selectivity. $\alpha = 0\%$, $\alpha = 50\%$, and $\alpha = 100\%$ respectively correspond to a cardioid, $\max-r_E$, and hyper-cardioid beampatterns. The figures are for the 3D case, with $N = 3$. The radial scale is logarithmic, with 6 dB per division.

3.3 UI and ergonomics

The two external objects `spat5.hoa.beamix~` and `spat5.hoa.beamix` benefit from the main ergonomic features introduced in version 5 of Spat [46]: (a) Communication is based on OSC messages and bundles offering inter-operability and flexibility of use; typically one can use pattern matching (for example the syntax `/beam/[10-20]`) simultaneously to send messages to several sectors; the `copy to neighbors` option (see \mathcal{C} on Figure 5) also allows one to propagate the settings of a zone to all adjacent sectors; more generally, it is possible to copy/paste the parameters from one sector to another. (b) It is easy to export/import/interpolate presets. (c) The audio engine is compatible with multichannel patchcords “MC” (see Figure 4), and highly optimized and vectorized. Nevertheless, user experience can still be improved; the two

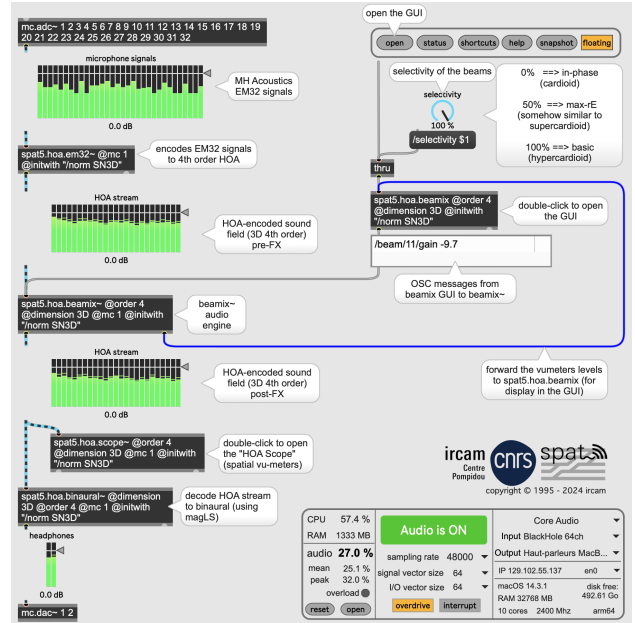


Figure 4. Example of a Max patch with `spat5.hoa.beamix~` processing a sound scene (here captured by an Ambisonics microphone, then rendered binaurally to headphones).

main challenges are due to the fact that (a) the tool operates in the space-time-frequency domain, where it is difficult to understand/visualize all dimensions simultaneously. (b) For higher orders N , the number of sectors is considerable and editing the scene quickly becomes tedious; it would therefore be useful to find efficient strategies for tweaking parameters either at the macro or micro level. There is no doubt that user feedback will help gradually to enrich the control interface and improve these aspects.

3.4 Discussion

The effects proposed in the processing chain (Figure 5, right panel) are (for the moment) quite basic; nevertheless, they offer a richer range of treatments than the other tools of the state of the art. In particular, non-linear processing (compressor/limiter) is very useful for correcting certain sound recordings, in order locally to emphasize sound elements that could be masked. Such non-linear FX cannot be applied directly in the SH domain because they would destroy the global spatial information; on the other hand, it is legitimate to use them locally on one or more sectors. In future work, we would like to enrich the range of available FX. For this, a relevant solution would be to insert existing (monophonic) plugins effects in each sector. Technically, this solution can already be implemented using Max’s `mc.vst~` object; however the operation is laborious, and native integration in `spat5.hoa.beamix~` could streamline the user workflow. The presence of a (monophonic) convolution engine on each sector already offers certain possibilities, however limited to the synthesis of linear and invariant systems. One possible application is the production of an artificial

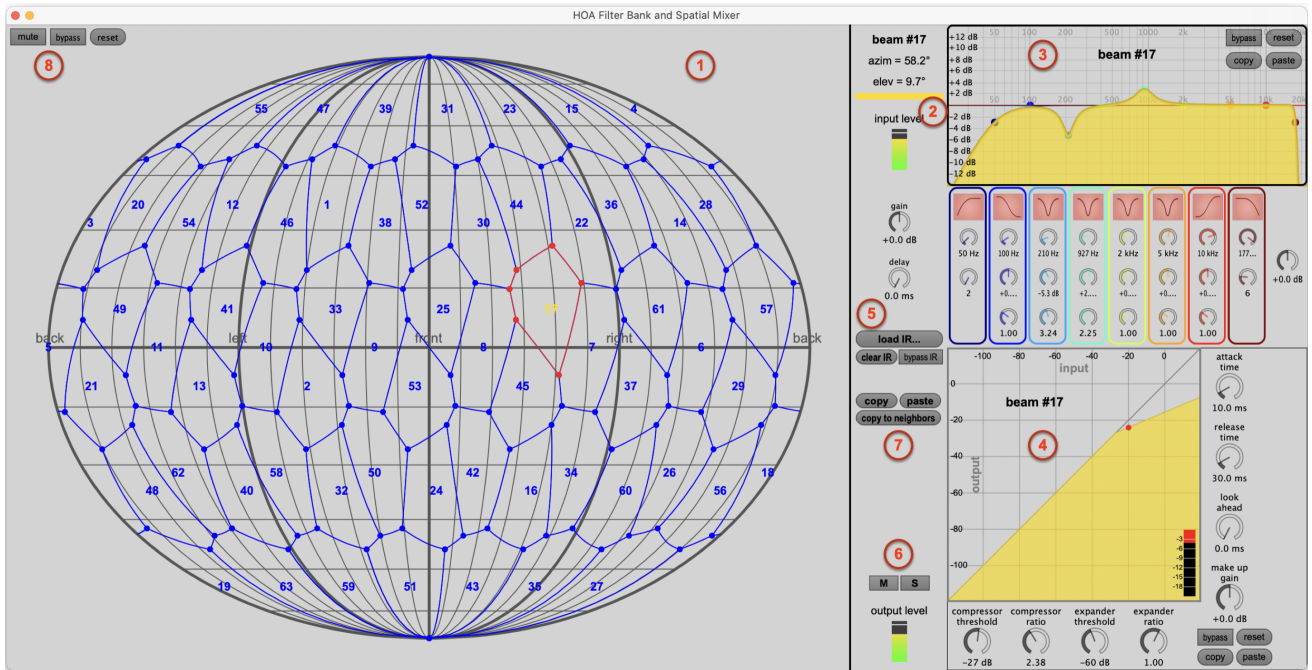


Figure 5. `spat5.hoa.beamix` GUI. Here in the 3D case, for order $N = 4$ and $K = 64$ beams. ① Cartographic projection of the sphere (here in Mollweide projection) and representation of the K angular sectors. ② Audio FX settings for the selected sector (here #17). ③ Equalizer for the selected sector. ④ Compressor and expander. ⑤ Button to load a finite impulse response filter. ⑥ Mute, solo, and output vu-meter for the selected sector. ⑦ Copy/paste the sector settings. ⑧ Global mute, bypass and reset controls (applied to all sectors).

reverberation effect whose characteristics (e.g. decay) vary depending on the directions [15]. However, it should be kept in mind that the calculation cost is likely to be considerable (in particular for “long” impulse responses) since it is proportional to the number K of sectors.

In addition to transforming sound scenes, another relevant use case concerns the editing of directional room impulse responses (DRIR) as captured by a spherical array of microphones. Once encoded in Ambisonics format, these responses can be edited locally, in the space-time-frequency domain, with `beamix`. This allows one, for example, to filter unwanted reflections, as already exemplified in [47]. It has also been shown that for DRIR exhibiting strong anisotropic characteristics, processing in the PWD can be more relevant than in the SH domain [12, 13]. The use of the Ambisonics filter bank is therefore appropriate for such responses. Finally, note that for editing DRIR, it is generally easier to work offline rather than in Max (or any other real-time oriented environment); this motivated the development of bindings of `beamix` for the command line (included in the `Spat` package) and for Matlab (currently not distributed publicly).

4. CONCLUSION

In this article we presented `beamix`, an audio engine and its graphical control interface allowing directional audio effects, i.e. FX localized in certain angular sectors. The effects are applied to an Ambisonics audio stream, previously

decomposed by a state-of-the-art spatial filter bank. The latter performs beamforming with virtual microphones and is analogous to a plane-wave decomposition. This approach allows greater flexibility compared to transformations applied in the modal domain. We presented the underlying mathematical formalism, then detailed the implementation of the tool, in particular its graphical interface which is intended to be intuitive and flexible.

However, several avenues for future improvement are considered. To enrich the arsenal of available FX, it would be relevant to allow the insertion of existing plugins (VST or other formats) in the processing chain. In addition, the ergonomics of the user interface can still be improved, and, in particular, it remains to invent strategies for joint editing (or visualization) of several neighboring sectors. And, more fundamentally, it remains for us to explore new approaches for the even more generic design of spatial filter banks, particularly in the wavelet domain [48], as this might offer adaptive spatial resolution depending on the areas of interest.

5. REFERENCES

- [1] U. Zölzer, *DAFX: Digital Audio Effects*, 2nd ed. John Wiley & Sons, March 2011. <https://doi.org/10.1002/9781119991298>
- [2] J. Benesty, J. Chen, and Y. Huang, *Microphone Array Signal Processing*. Springer, March 2008. <https://doi.org/10.1007/978-3-540-78612-2>

- [3] J. Benesty, J. Chen, and C. Pan, *Fundamentals of Differential Beamforming*. Springer, 2016. <https://doi.org/10.1007/978-981-10-1046-0>
- [4] J. Daniel, “Représentation de champs acoustiques, application à la transmission et à la reproduction de scènes sonores complexes dans un contexte multimédia,” Ph.D. dissertation, Université de Paris VI, September 2000. <https://www.theses.fr/2000PA066581>
- [5] F. Zotter and M. Frank, *Ambisonics: A Practical 3D Audio Theory for Recording, Studio Production, Sound Reinforcement, and Virtual Reality*, 1st ed. Cham, Switzerland: Springer, 2019. <https://doi.org/10.1007/978-3-030-17207-7>
- [6] B. Rafaely, “Spatial Sampling and Beamforming for Spherical Microphone Arrays,” in *Proc. of the Hands-Free Speech Communication and Microphone Arrays*, Trento, Italy, May 2008. <https://doi.org/10.1109/hscma.2008.4538673>
- [7] —, *Fundamentals of Spherical Array Processing*, 2nd ed. Cham, Switzerland: Springer, February 2019. <https://doi.org/10.1007/978-3-319-99561-8>
- [8] A. Politis and V. Pulkki, “Acoustic intensity, energy-density and diffuseness estimation in a directionally-constrained region,” *arXiv*, September 2016. <https://doi.org/10.48550/arXiv.1609.03409>
- [9] L. McCormack, S. Delikaris-Manias, A. Politis, D. Pavlidi, A. Farina, D. Pinaridi, and V. Pulkki, “Applications of Spatially Localized Active-Intensity Vectors for Sound-Field visualization,” *Journal of the Audio Engineering Society*, vol. 67, no. 11, pp. 840 – 854, November 2019. <https://doi.org/10.17743/jaes.2019.0041>
- [10] D. P. Jarrett, E. A. P. Habets, and P. A. Naylor, “3D source localization in the spherical harmonic domain using a pseudointensity vector,” in *Proc. of the 18th European Signal Processing Conference (EUSIPCO)*, Aalborg, Denmark, August 2010, pp. 442 – 446.
- [11] M. Nolan, E. Fernandez Grande, J. Brunskog, and C.-H. Jeong, “A wavenumber approach to quantifying the isotropy of the sound field in reverberant spaces,” *Journal of the Acoustical Society of America*, vol. 143, no. 4, pp. 2514–2526, 2018. <https://doi.org/10.1121/1.5032194>
- [12] P. Massé, T. Carpentier, O. Warusfel, and M. Noisternig, “Denoising Directional Room Impulse Responses with Spatially Anisotropic Late Reverberation Tails,” *Applied Sciences*, vol. 10, no. 3, pp. 1 – 17, February 2020. <https://doi.org/10.3390/app10031033>
- [13] —, “A robust denoising process for spatial room impulse responses with diffuse reverberation tails,” *Journal of the Acoustical Society of America*, vol. 147, no. 4, pp. 2250 – 2260, April 2020. <https://doi.org/10.1121/10.0001070>
- [14] M. Berzborn and M. Vorländer, “Directional sound field decay analysis in performance spaces,” *Building Acoustics*, vol. 28, no. 3, pp. 249 – 263, 2021. <https://doi.org/10.1177/1351010X20984622>
- [15] B. Alary, P. Massé, S. J. Schlecht, M. Noisternig, and V. Välimäki, “Perceptual analysis of directional late reverberation,” *Journal of the Acoustical Society of America*, vol. 149, no. 5, pp. 3189 – 3199, 2021. <https://doi.org/10.1121/10.0004770>
- [16] C. Hold, T. McKenzie, G. Götz, S. J. Schlecht, and V. Pulkki, “Resynthesis of Spatial Room Impulse Response Tails With Anisotropic Multi-Slope Decays,” *Journal of the Audio Engineering Society*, vol. 70, no. 6, pp. 526 – 538, June 2022. <https://doi.org/10.17743/jaes.2022.0017>
- [17] L. McCormack and A. Politis, “SPARTA & COMPASS: Real-time implementations of linear and parametric spatial audio reproduction and processing methods,” in *Proc. of the AES International Conference on Immersive and Interactive Audio*, York, UK, March 2019. <http://www.aes.org/e-lib/browse.cfm?elib=20417>
- [18] C. Hold, V. Pulkki, A. Politis, and L. McCormack, “Compression of Higher-Order Ambisonic Signals Using Directional Audio Coding,” *IEEE/ACM Transactions on Audio, Speech, and Language Processing*, vol. 32, pp. 651 – 665, 2024. <https://doi.org/10.1109/taslp.2023.3328284>
- [19] V. Pulkki, S. Delikaris-Manias, and A. Politis, *Parametric Time-Frequency Domain Spatial Audio*, V. Pulkki, S. Delikaris-Manias, and A. Politis, Eds. Wiley, October 2017. <https://doi.org/10.1002/9781119252634>
- [20] V. Pulkki, “Spatial Sound Reproduction with Directional Audio Coding,” *Journal of the Audio Engineering Society*, vol. 55, no. 6, pp. 503 – 516, June 2007. <http://www.aes.org/e-lib/browse.cfm?elib=14170>
- [21] S. Berge and N. Barrett, “High Angular Resolution Planewave Expansion,” in *Proc. of the 2nd International Symposium on Ambisonics and Spherical Acoustics*, Paris, France, May 2010.
- [22] A. Politis, J. Vilkamo, and V. Pulkki, “Sector-Based Parametric Sound Field Reproduction in the Spherical Harmonic Domain,” *IEEE Journal of Selected Topics in Signal Processing*, vol. 9, no. 5, pp. 852 – 866, August 2015. <https://doi.org/10.1109/jstsp.2015.2415762>
- [23] V. Pulkki, A. Politis, G. Del Galdo, and A. Kuntz, “Parametric Spatial Audio Reproduction with Higher-Order B-Format Microphone Input,” in *Proc. of the 134th Convention of the Audio Engineering Society (AES)*, Roma, Italy, May 2013. <http://www.aes.org/e-lib/browse.cfm?elib=16820>
- [24] C. Hold, L. McCormack, A. Politis, and V. Pulkki, “Optimizing Higher-Order Directional Audio Coding with Adaptive Mixing and Energy Matching for

- Ambisonic Compression and Upmixing,” in *Proc. of the IEEE Workshop on Applications of Signal Processing to Audio and Acoustics (WASPAA)*, New Paltz, NY, USA, October 2023. <https://doi.org/10.1109/waspaa58266.2023.10248179>
- [25] A. Wabnitz, N. Epain, A. McEwan, and C. Jin, “Upscaling Ambisonic sound scenes using compressed sensing techniques,” in *Proc. of the IEEE Workshop on Applications of Signal Processing to Audio and Acoustics (WASPAA)*, New Paltz, NY, USA, October 2011. <https://doi.org/10.1109/aspaa.2011.6082301>
- [26] A. Politis, S. Tervo, and V. Pulkki, “COMPASS: Coding and Multidirectional Parameterization of Ambisonic Sound Scenes,” in *Proc. of the IEEE International Conference on Acoustics, Speech and Signal Processing (ICASSP)*, Calgary, AB, Canada, April 2018, pp. 6802 – 6806. <https://doi.org/10.1109/icassp.2018.8462608>
- [27] C. Hold, S. J. Schlecht, A. Politis, and V. Pulkki, “Spatial Filter Bank in the Spherical Harmonic Domain: Reconstruction and Application,” in *Proc. of the IEEE Workshop on Applications of Signal Processing to Audio and Acoustics (WASPAA)*, New Paltz, NY, USA, October 2021. <https://doi.org/10.1109/waspaa52581.2021.9632709>
- [28] C. Hold, A. Politis, L. McCormack, and V. Pulkki, “Spatial Filter Bank Design in the Spherical Harmonic Domain,” in *Proc. of the European Signal Processing Conference (EUSIPCO)*, Dublin, Ireland, August 2021. <https://doi.org/10.23919/EUSIPCO54536.2021.9616091>
- [29] B. Rafaely, “Plane-wave decomposition of the sound field on a sphere by spherical convolution,” *Journal of the Acoustical Society of America*, vol. 116, no. 4, pp. 2149 – 2157, October 2004. <https://doi.org/10.1121/1.1792643>
- [30] M. Chapman and P. Cotterell, “Towards a comprehensive account of valid ambisonic transformations,” in *Proc. of the 1st Ambisonics Symposium*, Graz, Austria, 2009.
- [31] J. Daniel, “Evolving Views on HOA : From Technological To Pragmatic Concerns,” in *Proc. of the 1st Ambisonics Symposium*, Graz, Austria, June 2009.
- [32] M. Chapman, “Symmetries of Spherical Harmonics: Applications to Ambisonics,” in *Proc. of the 1st Ambisonics Symposium*, Graz, Austria, August 2009.
- [33] T. Carpentier, “Ambisonic spatial blur,” in *Proc. of the 142nd Convention of the Audio Engineering Society (AES)*, Berlin, Germany, May 2017. <https://www.aes.org/e-lib/browse.cfm?elib=18606>
- [34] M. Kronlachner and F. Zotter, “Spatial transformations for the enhancement of Ambisonic recordings,” in *Proc. of the 2nd International Conference on Spatial Audio (ICSA)*, Erlangen, Germany, February 2014.
- [35] M. A. Gerzon and G. J. Barton, “Ambisonic Decoders for HDTV,” in *Proc. of the 92nd Convention of the Audio Engineering Society (AES)*, Vienna, Austria, March 1992. <https://www.aes.org/e-lib/browse.cfm?elib=6788>
- [36] H. Pomberger and F. Zotter, “Warping of 3D ambisonic recordings,” in *Proc. of the Ambisonics Symposium*, Lexington, KY, USA, June 2011.
- [37] M. Hafsati, N. Epain, and J. Daniel, “Editing Ambisonic Sound Scenes,” in *Proc. of the 4th International Conference on Spatial Audio (ICSA)*, Graz, Austria, September 2017.
- [38] T. Carpentier, “Normalization schemes in Ambisonic: does it matter?” in *Proc. of the 142nd Convention of the Audio Engineering Society (AES)*, Berlin, Germany, May 2017.
- [39] N. A. Gumerov and R. Duraiswami, *Fast Multipole Methods for the Helmholtz Equation in Three Dimensions*, 1st ed. Elsevier, 2005. <https://doi.org/10.1016/b978-0-08-044371-3.x5000-5>
- [40] J. Meyer and G. W. Elko, “Spherical microphone arrays for 3d sound recording,” in *Audio Signal Processing for Next-Generation Multimedia Communication Systems*, Y. Huang and J. Benesty, Eds. Kluwer, 2004, ch. 3, pp. 67 – 89. https://doi.org/10.1007/1-4020-7769-6_3
- [41] R. H. Hardin and N. J. A. Sloane, “McLaren’s Improved Snub Cube and Other New Spherical Designs in Three Dimensions,” *Discrete & Computational Geometry*, vol. 15, no. 4, pp. 429 – 441, 1996. <https://doi.org/10.1007/bf02711518>
- [42] M. Gräf and D. Potts, “On the computation of spherical designs by a new optimization approach based on fast spherical Fourier transforms,” *Numerische Mathematik*, vol. 119, no. 4, pp. 699 – 724, 2011. <https://doi.org/10.1007/s00211-011-0399-7>
- [43] T. Carpentier, “Spherical beampatterns with fractional orders,” in *Proc. of the Forum Acusticum, 10th Convention of the European Acoustics Association (EAA)*, Torino, Italy, September 2023, pp. 607 – 614. <https://doi.org/10.61782/fa.2023.0531>
- [44] —, “Spat: a comprehensive toolbox for sound spatialization in Max,” *Ideas Sónicas*, vol. 13, no. 24, pp. 12 – 23, June 2021. <https://hal.science/hal-03356292>
- [45] T. Carpentier, O. Warusfel, and J.-M. Jot, “Software Tools for Flexible Control of Radiation Synthesis,” in *Proc. of the 2nd International Conference on Immersive and 3D Audio (I3DA)*, Bologna, Italy, September 2023. <https://doi.org/10.1109/I3DA57090.2023.10289260>
- [46] T. Carpentier, “A new implementation of Spat in Max,” in *Proc. of the 15th Sound and Music Computing Conference (SMC)*, Limassol, Cyprus, July 2018, pp. 184 – 191. <https://doi.org/10.5281/zenodo.1422552>

- [47] T. Carpentier, T. Szpruch, M. Noisternig, and O. Warusfel, "Parametric control of convolution based room simulators," in *Proc. of the International Symposium on Room Acoustics (ISRA)*, Toronto, Canada, June 2013. <https://hal.science/hal-01106836>
- [48] B. Yeo, W. Ou, and P. Golland, "On the Construction of Invertible Filter Banks on the 2-Sphere," *IEEE Transactions on Image Processing*, vol. 17, no. 3, pp. 283 – 300, March 2008. <https://doi.org/10.1109/tip.2007.915550>